RSC Advances

PAPER

View Article Online
View Journal | View Issue

Cite this: *RSC Adv.*, 2017, **7**, 33580

Eutypellazines A–M, thiodiketopiperazine-type alkaloids from deep sea derived fungus *Eutypella* sp. MCCC 3A00281†

Siwen Niu,[ab] Dong Liu,[a] Zongze Shao,*[b] Peter Proksch[c] and Wenhan Lin*[a]

Received 23rd May 2017
Accepted 27th June 2017

DOI: 10.1039/c7ra05774a

rsc.li/rsc-advances

Bioassay in association with the NMR/MS spectroscopic data guided fractionation of the solid fermentation of a deep sea derived fungus *Eutypella* sp. MCCC 3A00281, resulted in the isolation of 13 new thiodiketopiperazine-type alkaloids, namely eutypellazines A–M (**1–13**). Their structures were elucidated on the basis of extensive spectroscopic data analysis, including the ECD data, modified Mosher's method, and the Cu-Kα X-ray single-crystal diffraction experiments for the determination of the absolute configurations. An anti-HIV bioassay indicated that compounds **1–12** exhibited inhibitory effects against pNL4.3.Env-.Luc co-transfected 293T cells (HIV-1 model cells) with low cytotoxicity, of which eutypellazine E exerted the highest activity. A preliminary structure–activity relationship was discussed. In addition, eutypellazine J (**10**) and epicoccin A showed reactivating effects toward latent HIV-1 in J-Lat A2 cells.

1. Introduction

The natural thiodiketopiperazine alkaloids (TDKPs) are a class of unique fungal secondary metabolites, which are characterized by the presence of a diketopiperazine core featuring thiomethyl groups and/or transannular sulfide bridges.[1–6] The TDKP derivatives are biogenetically derived from at least one aromatic amino acid (phenylalanine, tryptophan or tyrosine), while the unusual sulfur bridges and thiomethyl units are generated by the mediation of biosynthetic genes such as glutathione S-transferase.[7,8] TDKP derivatives are widely distributed in diverse fungal genera, whereas the fungal strains, belonging to the genera of *Penicillium*,[6] *Exserohilum*,[9] and *Phoma*,[10] from marine inhabitation are the rich sources to derive TDKP analogues. So far, an array of TDKPs with diverse scaffolds due to the formation of different amino acids or distinct sulfur bridges has been found from fungal origin, and the structural variety directly affected their bioactivity. The biological activities are mainly focused on cytotoxic,[9,11] antibacterial,[12,13] antiangiogenic,[14] anti-inflammatory,[15] and antituberculosis.[16] In continuation of our research program aiming the discovery of bioactive metabolites from deep-sea derived microorganisms, the EtOAc extract of the fermentation of a deep-sea derived fungus *Eutypella* sp. MCCC 3A00281 exhibited inhibitory effect against HIV-1 virus (Table 1). Chromatographic fractionation of the active extract in association with the bioassay and NMR/ESIMS experiments revealed that the active fractions F7 and F8 featured a profile of thiodiketopiperazine-type derivatives. Further chromatographic separation of both F7 and F8 fractions resulted in the isolation of 15 TDKP derivatives, including 13 new analogues namely eutypellazines A–M (**1–13**) (Fig. 1). In this paper, we intend to report the structure elucidation of new compounds and their anti-HIV-1 activities.

2. Experimental section

2.1. General procedure

Melting points were measured on X-5 micromelting-point apparatus. IR spectra were determined by a Thermo Nicolet

Table 1 Inhibitory effects of the fractions toward HIV-1[a]

Fractions	c (μg mL^{-1})	Inhibitory rates (%)
EtOAc extract	10	46.3
F3	10	0
F4	10	9.7
F5	10	29.4
F6	10	5.1
F7	10	99.6
F8	10	68.6
F9	10	46.0
F10	10	18.0
EFV	0.1 (μM)	96.22

[a] EFV (Efavirenz): positive control, bioassay was performed in pNL4.3.Env-.Luc co-transfected 293T cells.

[a]*State Key Laboratory of Natural and Biomimetic Drugs, Peking University, Beijing, 100191, P. R. China. E-mail: whlin@bjmu.edu.cn; Fax: +86-10-82806188*

[b]*Key Laboratory of Marine Biogenetic Resources, Third Institute of Oceanography, SOA, Xiamen, 361005, P. R. China*

[c]*Institute of Pharmaceutical Biology and Biotechnology, Heinrich-Heine University, 40225 Duesseldorf, Germany*

† Electronic supplementary information (ESI) available. CCDC 1416589–1416593. For ESI and crystallographic data in CIF or other electronic format see DOI: 10.1039/c7ra05774a

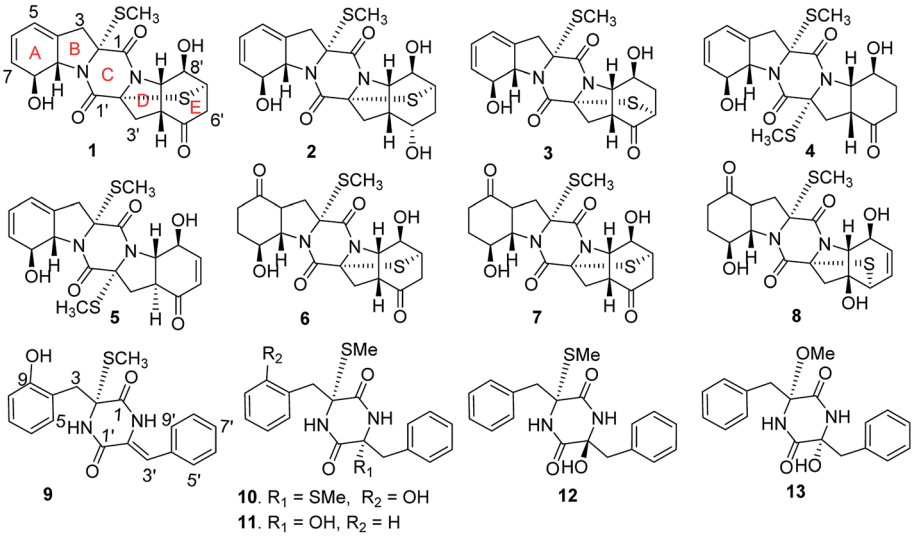

Fig. 1 Structures of new compounds.

Nexus 470 FT-IR spectrometer. UV spectra were measured on a Cary 300 spectrometer. Optical rotations were obtained from a Rudolph IV Autopol automatic polarimeter at 25 °C. CD spectra were measured on a JASCO J-810 spectropolarimeter. NMR spectra were recorded on Bruker Advance 400 MHz spectrometers. Chemical shifts are expressed in δ (ppm) referenced to the solvent peaks at δ_H 2.50/δ_C 39.5 for DMSO-d_6 and δ_H 7.26/δ_C 77.2 for $CDCl_3$, and coupling constants (J) are in Hz. HRESIMS spectra were obtained from Xevo G2 Q-TOF mass spectrometer (Waters). X-ray data were obtained by a Bruker D8 Advance single crystal X-ray diffractometer using graphite monochromated Cu-Kα radiation. Column chromatography (CC) was performed by silica gel (100–200 and 200–300 mesh, Qingdao Marine Chemistry Co. Ltd. China), ODS gel (50 μm, YMC, Japan) and Sephadex LH-20 (18–110 μm, Amersham Pharmacia Biotech AB, Uppsala, Sweden). The precoated silica gel plates (Merck, Kieselgel 60 F254, 0.25 mm) were used for TLC analysis. HPLC chromatography was performed on a Waters e2695 separation Module coupled with a Waters 2998 photodiode array detector, and a semi-preparative reversed-phased column (YMC-packed C18, 5 μm, 250 mm × 10 mm) was used for purification. 293T cells (ATCC® CRL-3216™) from embryonic kidney of human were provided from American Type Culture Collection (ATCC). J-lat-A2 cells were provided by the Verdin laboratory (Buck Institute, CA), and were generated by transduction of Jurkat T cells (NIH AIDS Reagent Program) with an HIV vector expressing Tat-Flag and GFP under the control of the viral 5′-LTR and IRES positioned in between Tat and GFP (LTR-Tat-Flag-IRES-GFP).

2.2. Fungal material and fermentation

The fungus *Eutypella* sp. MCCC 3A00281 was isolated from the deep sea sediment, collected with TV-multicore from South Atlantic Ocean (GPS 27.90 W, 6.43 S) at the depth of 5610 meters during the Comra 22nd oceanic cruise in June 2011. On the basis of the rRNA analysis, the genus of *Eutypella* was determined (GeneBank accession number KT366012). The strain was deposited in the Marine Culture Collection of China (MCCC), Third Institute of Oceanography, State Oceanic Administration (SOA), Xiamen, China.

The fungal strain MCCC 3A00281 was cultured on the slants of PDA medium at 25 °C for 6 days. The fresh mycelia were cut and inoculated to 45 × 500 mL Erlenmeyer flasks, each flask contains 100 g rice and 140 mL distilled water. After autoclaving at 15 psi for 30 min, these flasks were inoculated and incubated at room temperature for 25 days. The fermented fungal material was extracted with EtOAc for three times, and then concentrated under *vacuo* to afford crude extract.

2.3. Isolation and purification

The EtOAc extract was tested by the pNL4.3.Env-.Luc co-transfected 293T cells (HIV-1 model cells) showing 46% inhibitory rate in a dose of 10 μg mL^{-1}. The active extract (13 g) was subjected to a silica gel vacuum liquid chromatography (VLC), eluting with a gradient of petroleum ether (PE) and acetone (1 : 0 to 0 : 1) to yield 10 fractions (F1–F10). Fractions F1 to F4 (sum amount 4.3 g) were detected by the ^{1}H NMR spectra to show the resonances mainly containing fatty acids. Fractions F5 and F6 (sum amount 2.0 g) featured terpenoid resonances in the ^{1}H NMR spectra. The polar fractions F9 and F10 (sum amount 5.4 g) displayed the resonances for polyphenols and saccharides in the ^{1}H NMR spectra. In addition, the ^{1}H NMR and ESIMS spectra of F7 and F8 (sum amount 1.0 g) displayed the metabolite profile of thiodiketopiperazine alkaloids. Bioassay of the fractions F3 to F10 using pNL4.3.Env-.Luc co-transfected 293T cells (HIV-1 model cells) revealed that F7 and F8 possess potential inhibition against HIV-1 virus, of which F7 showed the most active (Table 1). Fraction F7 (0.4 g) was subjected to ODS column chromatography (CC) eluting with a gradient with increasing MeOH in H_2O (30% to 100%) to afford 11 subfractions (SF71–SF711). The HPLC fingerprints of SF71–SF76 were overlapped with that of inactive fraction F6. SF77 (112 mg) was separated by

the semi-preparative HPLC with a mobile phase of MeCN–H_2O (3 : 2) to obtain **5** (13.4 mg), **10** (2.8 mg), **4** (46.6 mg), and **9** (2.3 mg). SF78 (157 mg) was separated by the semi-preparative HPLC with a mobile phase of MeCN–H_2O (7 : 13) to obtain **13** (15.8 mg) and **12** (4.5 mg). F8 (0.5 g) was fractionated upon an ODS column chromatography using a gradient elution of MeOH in H_2O (20–100%) to afford 15 subfractions (SF81–SF815). SF86 (101 mg) was separated by the semi-preparative HPLC (MeCN–H_2O, 1 : 3) to afford epicoccin A (42.3 mg), **6** (28.8 mg), and **7** (14.2 mg), while **8** (2.5 mg) from SF88 (MeCN–H_2O = 7 : 18), **2** (3.5 mg) from SF89 (MeOH/H_2O = 43 : 57), and **1** (47.5 mg) from SF811 (MeCN/H_2O = 27 : 73) were separated by the semi-preparative HPLC chromatography. SF812 (135 mg) was subjected to silica gel CC eluted with CH_2Cl_2–MeOH (50 : 1) to yield **3** (12.7 mg), epicoccin I (10.6 mg), and **11** (2.6 mg).

Eutypellazine A (1). Monoclinic crystal; mp 267–269 °C; $[\alpha]_D^{25}$ +160 (*c* 0.2, MeOH); UV (MeOH) λ_{max} (log ε) 202 (4.11) and 264 (3.55) nm; CD (MeOH) λ_{max} ($\Delta\varepsilon$) 267 (+5.45), 246 (+7.10), 205 (+20.13) nm; IR (KBr) ν_{max} 3370, 2922, 1713, 1647, 1418, 1324, 1230, 1190 cm^{-1}; ^1H and ^{13}C NMR data, see Tables 2 and 4; HRESIMS *m*/*z* 421.0887 $[M + H]^+$ (calcd for $C_{19}H_{21}N_2O_5S_2$, 421.0892).

Eutypellazine B (2). White powder; $[\alpha]_D^{25}$ +140 (*c* 0.1, MeOH); UV (MeOH) λ_{max} (log ε) 204 (4.01), 265 (3.06) nm; CD (MeOH) λ_{max} ($\Delta\varepsilon$) 264 (+6.78), 245 (+5.45), 220 (+9.58), 201 (+11.38) nm; IR (KBr) ν_{max} 3392, 2920, 1697, 1649, 1416, 1232 cm^{-1}; ^1H and ^{13}C NMR data, see Tables 2 and 4; HRESIMS *m*/*z* 423.1043 $[M + H]^+$ (calcd for $C_{19}H_{23}N_2O_5S_2$, 423.1048).

Eutypellazine C (3). White powder; $[\alpha]_D^{25}$ +277 (*c* 0.2, MeOH); UV (MeOH) λ_{max} (log ε) 204 (4.18), 266 (3.59) nm; CD (MeOH) λ_{max} ($\Delta\varepsilon$) 307 (+8.45), 248 (−3.19), 213 (+16.65) nm; IR (KBr) ν_{max} 3366, 2921, 1706, 1648, 1418, 1230 cm^{-1}; ^1H and ^{13}C NMR data, Tables 2 and 4; HRESIMS *m*/*z* 421.0888 $[M + H]^+$ (calcd for $C_{19}H_{21}N_2O_5S_2$, 421.0892).

Eutypellazine D (4). White powder; $[\alpha]_D^{25}$ −101 (*c* 0.5, MeOH); UV (MeOH) λ_{max} (log ε) 205 (4.10), 261 (3.59) nm; CD (MeOH) λ_{max} ($\Delta\varepsilon$) 284 (+1.60), 262 (−3.72), 237 (+4.33), 212 (−8.36) nm; IR (KBr) ν_{max} 3379, 2923, 1706, 1637, 1414, 1328, 1237, 1201 cm^{-1}; ^1H and ^{13}C NMR data, see Tables 2 and 4; HRESIMS *m*/*z* 437.1201 $[M + H]^+$ (calcd for $C_{20}H_{25}N_2O_5S_2$, 437.1205).

Eutypellazine E (5). Orthorhombic crystal; mp 242–244 °C; $[\alpha]_D^{25}$ −154 (*c* 0.5, MeOH); UV (MeOH) λ_{max} (log ε) 207 (4.16), 264 (3.55) nm; CD (MeOH) λ_{max} ($\Delta\varepsilon$) 289 (+1.59), 256 (−2.48), 248 (−2.27), 215 (−31.04) nm; IR (KBr) ν_{max} 3351, 2922, 1692, 1639, 1412, 1374, 1262, 1185, 1125 cm^{-1}; ^1H and ^{13}C NMR data, see Tables 2 and 4; HRESIMS *m*/*z* 435.1049 $[M + H]^+$ (calcd for $C_{20}H_{23}N_2O_5S_2$, 435.1048).

Eutypellazine F (6). Orthorhombic crystal; mp 208–210 °C; $[\alpha]_D^{25}$ +84 (*c* 1.0, MeOH); UV (MeOH) λ_{max} (log ε) 207 (4.33) nm; IR (KBr) ν_{max} 3396, 2922, 1709, 1655, 1419, 1362, 1324, 1225 cm^{-1}; ^1H and ^{13}C NMR data, see Tables 3 and 4; HRESIMS *m*/*z* 439.0995 $[M + H]^+$ (calcd for $C_{19}H_{23}N_2O_6S_2$, 439.0998).

Eutypellazine G (7). Orthorhombic crystal; mp 204–206 °C; $[\alpha]_D^{25}$ +120 (*c* 0.5, MeOH); UV (MeOH) λ_{max} (log ε) 204 (4.19) nm; IR (KBr) ν_{max} 3392, 2923, 1707, 1653, 1420, 1324 cm^{-1}; ^1H and ^{13}C NMR data, see Tables 3 and 4; HRESIMS *m*/*z* 441.1151 $[M + H]^+$ (calcd for $C_{19}H_{25}N_2O_6S_2$, 441.1154).

Eutypellazine H (8). Orthorhombic crystal; mp 298–300 °C; $[\alpha]_D^{25}$ +134 (*c* 0.2, MeOH); UV (MeOH) λ_{max} (log ε) 206 (4.16) nm; IR (KBr) ν_{max} 3363, 2923, 1703, 1648, 1414, 1241 cm^{-1}; ^1H and ^{13}C NMR data, see Tables 3 and 4; HRESIMS *m*/*z* 439.1000 $[M + H]^+$ (calcd for $C_{19}H_{23}N_2O_6S_2$, 439.0998).

Eutypellazine I (9). White powder; $[\alpha]_D^{25}$ −94 (*c* 0.1, MeOH); UV (MeOH) λ_{max} (log ε) 202 (4.09), 300 (3.74) nm; IR (KBr) ν_{max}

Table 2 ^1H NMR data of compounds **1–5** in DMSO-d_6

Position	1	2	3	4	5
3	3.03, d (14.0); 3.05, d (14.0)	3.01, d (14.0); 3.04 d (14.0)	3.01, d (14.0); 3.05 (14.0)	3.00, d (14.0); 3.04, d (14.0)	2.98, d (15.5); 3.06, d (15.5)
5	5.98, d (4.5)	5.97, d (4.5)	5.98, d (4.5)	5.96, d (4.5)	5.99, d (4.5)
6	5.91, dd (10.0, 4.5)	5.90, dd (10.0, 4.5)	5.91, dd (9.8, 4.5)	5.89, dd (9.8, 4.5)	5.91, dd (9.8, 4.5)
7	5.62, brd (10.0)	5.62, d (10.0)	5.62, brd (9.8)	5.62, brd (9.8)	5.65, brd (9.8)
8	4.66, brd (13.8)	4.65, brd (13.9)	4.60, brd (13.6)	4.58, brd (13.3)	4.63, d (13.8)
9	4.78, d (13.8)	4.77, d (13.9)	4.76, d (13.6)	4.70, d (13.3)	4.75, d (13.8)
3′	2.76, d (13.1) 2.98, dd (13.1, 8.5)	2.59, dd (13.0, 8.5) 2.79, dd (13.0, 1.5)	2.88, d (11.6) 3.07, dd (11.6, 7.0)	2.31, dd (13.2, 7.8) 2.83, d (13.2)	2.29, t (12.7) 2.44, dd (12.7, 5.0)
4′	3.03, dd (11.5, 8.0)	2.69, dt (8.5, 8.0)	3.16, t (7.0)	3.00, dd (8.0, 7.8)	3.42, dt (13.3, 5.0)
5′		4.31, m			
6′	2.92, dd (18.8, 7.5) 3.12, d (18.8)	1.97, dd (14.6, 7.8) 2.74, m	3.64, d (8.9)	2.24, ddd (12.0, 6.0, 8.0) 2.63, dt (12.0, 7.0)	6.06, dd (10.2, 2.0)
7′	3.74, dd (7.5, 5.8)	3.39, dd (8.2, 3.8)	2.53, dd (15.4, 8.9) 2.69, dd (15.4, 4.5)	1.92, m 2.19, m	6.91, dd (10.2, 1.7)
8′	4.03, ddd (5.8, 4.0, 2.5)	3.85, brdd (4.0, 3.8)	4.50, t (4.5)	4.37, brt (4.0)	4.57, brd (8.7)
9′	4.78, dd (8.0, 5.8)	4.49, ddd (8.0, 4.0)	4.62, dd (7.0, 4.5)	4.35, dd (8.0, 4.0)	3.83, dd (13.3, 8.7)
CH_3S-2	2.24, s	2.21, s	2.20, s	2.12, s	2.19, s
CH_3S-2′				1.97, s	2.17, s
OH-8	5.43, d (1.2)	5.53, br	5.35, br	5.31, br	5.17, d (2.0)
OH-5′		4.85, d (4.6)			
OH-8′	6.21, d (2.5)	5.91, br	5.56, br	5.37, br	6.18, br

Table 3 ^{1}H NMR data of **6–13** in DMSO-d_6 (400 MHz)

Position	6	7	8	9	10	11	12	13
3	2.32, dd (13.5, 8.5)	2.29, dd (13.6, 8.3)	2.39, dd (13.6, 8.3)	3.18, d (14.4)	3.01, d (15.7)	2.84, d (13.6)	2.68, d (12.7)	2.78, d (13.1)
	2.86, d (13.5)	2.85, d (13.6)	2.76, d (13.6)	3.46, d (14.4)	3.09, d (15.7)	3.21, d (13.6)	3.27, d (12.7)	3.09, d (13.1)
4	3.06, t (8.5)	3.04, dd (8.3, 8.0)	2.98, t (8.3)					
5				7.12, d (7.6)	6.30, dd (7.5, 1.6)	7.04, d (8.0)	7.20, d (8.0)	7.12, d (8.0)
6	2.26, dt (17.7, 4.6)	2.25, m	2.21, dt (17.6, 4.8)	6.70, t (7.6)	6.25, t (7.5)	7.07, t (8.0)	7.20, t (8.0)	7.20, t (8.0)
	2.59, m	2.57, m	2.58, m					
7	1.91, m; 2.12, m	1.90, m; 2.10, m	1.87, m; 2.03, m	7.04, t (7.6)	6.89, t (7.5)	7.00, t (8.0)	7.20, t (8.0)	7.15, t (8.0)
8	4.33, br	4.30, dt (3.8, 2.1)	4.30, brt (3.4)	6.81, d (7.6)	6.67, d (7.5)	7.07, t (8.0)	7.20, t (8.0)	7.20, t (8.0)
9	4.39, dd (8.5, 3.8)	4.39, d (8.0, 3.8)	4.37, dd (8.3, 3.4)			7.04, d (8.0)	7.20, d (8.0)	7.12, d (8.0)
3′	2.71, d (13.4)	2.53, dd (12.8, 8.0)	2.57, (12.6, 8.0)	6.62, s	2.97, d (13.6)	2.65, d (13.3)	2.86, d (13.2)	2.68, d (12.7)
	2.91, dd (13.4, 8.0)	2.74, d (12.8)	2.68, d (12.6)		3.48, d (13.6)	2.90, d (13.3)	3.32, d (13.2)	3.27, d (12.7)
4′	3.00, dd (8.0, 7.9)	2.67, dt (8.0, 4.0)						
5′		4.28, m	4.17, dd (6.2, 1.5)	7.47, d (7.6)	7.14, d (8.0)	6.89, d (7.4)	7.08, d (8.0)	7.20, d (8.0)
6′	2.89, dd (15.7, 5.3)	1.94, m	5.98, ddd (10.2, 6.2)	7.38, t (7.6)	7.14, t (8.0)	6.96, t (7.4)	7.18, t (8.0)	7.20, t (8.0)
	3.09, d (15.7)	2.72, m						
7′	3.70, t (5.3)	3.35, t (5.0)	5.76, ddd (10.2, 3.5, 1.5)	7.29, t (7.6)	7.17, t (8.0)	7.04, t (7.4)	7.20, t (8.0)	7.20, t (8.0)
8′	4.00, brdd (5.3, 4.0)	3.83, ddd (5.0, 4.0, 3.2)	4.42, brd (3.5)	7.38, t (7.6)	7.14, t (8.0)	6.96, t (7.4)	7.18, t (8.0)	7.20, t (8.0)
9′	4.70, dd (7.9, 4.0)	4.41, dd (8.5, 4.0)	3.96, brs	7.47, d (7.6)	7.14, d (8.0)	6.89, d (7.4)	7.08, d (8.0)	7.20, d (8.0)
SMe-2	2.04, s	2.01, s	1.92, s	2.20, s	2.21, s	2.20, s	1.19, s	
SMe-2′					2.30, s			
OMe-2								2.06, s
OH-8	5.40, br	5.39, d (2.1)	5.39, br					
OH-4′			6.14, s				5.76, s	5.85, s
OH-5′		4.81, d (4.9)						
OH-8′	6.20, br	5.86, d (3.2)	5.09, br					
OH-9				10.21, s	9.37, s			
NH-1				9.84, br s	9.03, s	8.68, s	8.67, s	8.94, s
NH-1′				8.55, br s	8.42, s	8.52, s	8.58, s	8.40, s

3734, 2921, 1670, 1448, 1417, 1375, 1237 cm^{-1}; ^{1}H and ^{13}C NMR data, see Tables 3 and 4; HRESIMS *m*/*z* 355.1120 $[M + H]^+$ (calcd for $C_{19}H_{19}N_2O_3S$, 355.1116).

Eutypellazine J (10). White powder; $[\alpha]_D^{25}$ −128 (*c* 0.1, MeOH); UV (MeOH) λ_{max} (log ε) 203 (4.19), 276 (2.83) nm; IR (KBr) ν_{max} 3180, 2921, 1838, 1663, 1847, 1435, 1369, 1228 cm^{-1}; ^{1}H and ^{13}C NMR data, see Tables 3 and 4; HRESIMS *m*/*z* 425.0965 $[M + Na]^+$ (calcd for $C_{20}H_{22}N_2O_3S_2Na$, 425.0970).

Eutypellazine K (11). White powder; $[\alpha]_D^{25}$ −165 (*c* 0.05, MeOH); UV (MeOH) λ_{max} (log ε) 202 (4.11) nm; IR (KBr) ν_{max} 3412, 3292, 3207, 1671, 1495, 1436, 1242, 1109 cm^{-1}; ^{1}H and ^{13}C NMR data, see Tables 3 and 4; HRESIMS *m*/*z* 355.1112 $[M - H]^-$ (calcd for $C_{19}H_{19}N_2O_3S$, 355.1116).

Eutypellazine L (12). White powder; $[\alpha]_D^{25}$ −80 (*c* 0.02, MeOH); UV (MeOH) λ_{max} (log ε) 202 (4.01) nm; IR (KBr) ν_{max} 3275, 3204, 1672, 1496, 1453, 1437, 1403, 1307, 1240 cm^{-1}; ^{1}H and ^{13}C NMR data, see Tables 3 and 4; HRESIMS *m*/*z* 355.1120 $[M - H]^-$ (calcd for $C_{19}H_{19}N_2O_3S$, 355.1116).

Eutypellazine M (13). White powder; $[\alpha]_D^{25}$ −72 (*c* 0.05, MeOH); UV (MeOH) λ_{max} (log ε) 205 (4.08) nm; IR (KBr) ν_{max} 3430, 3289, 3206, 1668, 1495, 1435, 1405, 1110 cm^{-1}; ^{1}H and ^{13}C NMR data, see Tables 3 and 4; HRESIMS *m*/*z* 339.1342 $[M - H]^-$ (calcd for $C_{19}H_{19}N_2O_4$, 339.1345).

2.4. Preparation of (*R*)-MPA and (*S*)-MPA esters of 4

Compound **4** (2.0 mg for each) was dissolved in $CHCl_3$ (600 μL) and (*R*)-MPA (3.0 mg), DMAP (2.8 mg) and DCC (2.5 mg) were added. The mixture was kept at room temperature for 12 h. The reaction products were purified by silica gel CC eluted with PE : acetone (5 : 1) to get bis-(*R*)-MPA ester **4a** (1.8 mg). In an identical protocol, bis-(*S*)-MPA ester of **4b** (2.1 mg) was obtained from **4**.

Bis-(*R*)-MPA ester of 4 (4a). ^{1}H NMR ($CDCl_3$, 400 MHz) δ_H 7.34–7.47 (10H, m, phenyl protons), 5.93–5.97 (3H, m, H-5/H-6/H-8), 5.76 (1H, brs, H-8′), 5.58 (1H, m, H-7), 5.31 (1H, d, J = 12.8 Hz, H-9), 4.82 (1H, s, CH of MPA), 4.79 (1H, s, CH of MPA),

Table 4 ^{13}C NMR data of **1–13** in DMSO-d_6

No.	1	2	3	4	5	6	7	8	9	10	11	12	13
1	159.5, C	159.5, C	162.1, C	165.7, C	169.2, C	159.8, C	159.9, C	161.4, C	164.7, C	166.3, C	166.0, C	166.1, C	165.0, C
2	74.7, C	74.6, C	74.6, C	74.0, C	73.7, C	72.5, C	72.4, C	72.2, C	67.6, C	65.2, C	67.2, C	68.6, C	87.4, C
3	38.3, CH_2	38.3, CH_2	38.1, CH_2	38.3, CH_2	38.2, CH_2	34.2, CH_2	34.3, CH_2	34.9, CH_2	36.6, CH_2	37.1, CH_2	43.7, CH_2	44.4, CH_2	45.1, CH_2
4	134.1, C	134.2, C	134.0, C	134.3, C	134.0, C	44.9, CH	44.9, CH	44.5, CH	122.3, C	122.3, C	135.2, C	135.3, C	134.5, C
5	119.6, CH	119.5, CH	120.0, CH	119.4, CH	119.6, CH	207.7, C	207.7, C	208.2, C	131.7, CH	130.0, CH	130.5, CH	131.2, CH	131.1, CH
6	123.9, CH	123.8, CH	123.9, CH	123.8, CH	124.0, CH	34.5, CH_2	34.5, CH_2	34.4, CH_2	119.5, CH	119.4, CH	128.2, CH	128.3, CH	128.3, CH
7	131.0, CH	130.9, CH	131.0, CH	130.9, CH	131.4, CH	26.4, CH_2	26.4, CH_2	26.2, CH_2	128.6, CH	127.7, CH	127.1, CH	127.1, CH	127.1, CH
8	73.9, CH	74.0, CH	74.1, CH	74.2, CH	74.3, CH	65.5, CH	65.9, CH	64.8, CH	115.7, CH	115.2, CH	128.2, CH	128.3, CH	128.3, CH
9	69.3, CH	69.3, CH	69.2, CH	68.3, CH	68.0, CH	66.5, CH	66.5, CH	66.5, CH	156.0, C	155.6, C	130.5, CH	131.2, CH	131.1, CH
1′	165.9, C	167.0, C	165.2, C	168.1, C	167.2, C	164.1, C	165.1, C	163.1, C	160.9, C	165.6, C	167.5, C	167.0, C	167.6, C
2′	70.1, C	69.2, C	72.8, C	71.7, C	72.8, C	70.1, C	69.2, C	73.4, C	125.8, C	65.5, C	81.9, C	82.7, C	82.8, C
3′	44.8, CH_2	43.1, CH_2	53.3, CH_2	34.6, CH_2	31.7, CH_2	44.6, CH_2	42.9, CH_2	54.1, CH_2	115.3, CH	43.5, CH_2	44.8, CH_2	44.3, CH_2	44.8, CH_2
4′	45.3, CH	39.1, CH	46.1, CH	44.4, CH	46.4, CH	45.4, CH	39.1, CH	77.5, C	133.5, C	135.5, C	135.1, C	135.8, C	135.7, C
5′	207.9, C	61.5, CH	205.6, C	207.9, C	196.6, C	208.1, C	61.6, CH	43.8, CH_2	129.8, CH	130.8, CH	130.4, CH	131.1, CH	131.2, CH
6′	42.1, CH_2	37.3, CH_2	45.7, CH	34.3, CH_2	128.6, CH	42.1, CH_2	37.3, CH_2	127.7, CH	129.2, CH	128.4, CH	128.1, CH	128.3, CH	128.3, CH
7′	41.8, CH	42.4, CH	41.5, CH_2	26.4, CH_2	152.7, CH	41.8, CH	42.4, CH	128.9, CH	128.6, CH	127.2, CH	126.7, CH	127.2, CH	127.1, CH
8′	66.1, CH	68.0, CH	62.1, CH	64.1, CH	72.7, CH	65.6, CH	67.5, CH	62.4, CH	129.2, CH	128.4, CH	128.1, CH	128.3, CH	128.3, CH
9′	60.3, CH	57.6, CH	63.5, CH	65.5, CH	69.1, CH	60.2, CH	57.6, CH	66.0, CH	129.8, CH	130.8, CH	130.4, CH	131.1, CH	131.2, CH
SMe-2	14.5, CH_3	14.5, CH_3	14.3, CH_3	14.5, CH_3	14.6, CH_3	14.6, CH_3	14.6, CH_3	14.2, CH_3	13.4, CH_3	13.9, CH_3	13.5, CH_3	11.4, CH_3	
SMe-2′				15.0, CH_3	15.0, CH_3					14.0, CH_3			
MeO-2													49.1, CH_3

4.45 (1H, d, $J = 7.8$ Hz, H-9′), 3.52 (3H, OMe of MPA), 3.46 (3H, OMe of MPA), 3.07 (1H, d, $J = 13.9$ Hz, H-3′a), 3.02 (1H, d, $J = 16.2$ Hz, H-3a), 2.85 (1H, d, $J = 16.2$ Hz, H-3b), 2.75 (1H, t, $J = 7.8$ Hz, H-4′), 2.32 (1H, m, H-7′a), 2.25 (1H, m, H-6′a), 2.21 (3H, s, SMe-2), 2.13 (1H, dd, $J = 7.8$, 14.1 Hz, H-3′b), 2.02 (1H, m, H-7′b), 1.82 (1H, m, H-6′b), 1.80 (3H, s, SMe-2′).

Bis-(*S*)-MPA ester of 4 (4b). ^{1}H NMR ($CDCl_3$, 400 MHz) δ_H 7.33–7.47 (10H, m, phenyl protons), 5.92–5.97 (3H, m, H-5/H-6/H-8), 5.84 (1H, brs, H-8′), 5.58 (1H, m, H-7), 5.27 (1H, d, $J = 13.2$ Hz, H-9), 4.82 (1H, s, CH of MPA), 4.78 (1H, s, CH of MPA), 4.23 (1H, d, $J = 7.6$ Hz), 3.51 (3H, OMe of MPA), 3.46 (3H, OMe of MPA), 3.01 (1H, d, $J = 14.1$ Hz, H-3′a), 3.00 (1H, d, $J = 16.1$ Hz, H-3a), 2.82 (1H, d, $J = 16.1$ Hz, H-3b), 2.47 (1H, m, H-7′a), 2.43 (2H, m, H-4′/H-6′a), 2.36 (1H, m, H-6′b), 2.19 (3H, s, SMe-2), 2.18 (1H, m, H-7′b), 2.04 (1H, dd, $J = 7.8$, 14.1 Hz, H-3′b), 1.77 (3H, s, SMe-2′).

2.5. X-ray single crystal diffraction

Eutypellazine A (**1**) was obtained colorless crystal from MeOH/H_2O (50 : 1) using the vapor diffusion method. The monoclinic crystal (0.06 × 0.04 × 0.03) was measured on Bruker D8 Advance single crystal X-ray diffractometer with Cu-Kα radiation at 104.7 K. Crystal data of **1**: empirical formula $C_{19}H_{22}N_2O_6S_2$, $M = 438.51$; space group $P2_1$, unit cell dimensions $a = 7.6255$ (4) Å, $b = 27.2984(13)$ Å, $c = 9.2094(5)$ Å, $\alpha = \gamma = 90.00°$, $\beta = 90.415(5)°$, $V = 1917.01(17)$ Å, $Z = 4$, $D_{calcd} = 1.1519$ mg m^{-3}, $\mu = 2.886$ mm^{-1}, $F(000) = 920$; a total of 13 001 reflections were collected in the range of $6.48° < 2\theta < 142.48°$, of which 7261 independent reflections [$R_{(int)} = 0.0486$ (inf-0.9 Å)] were used for the analysis. The structure was solved by the direct methods with the SHELXL-97 program and refined using full-matrix least-squares difference Fourier techniques. The final R indexes [all data] gave $R_1 = 0.0484$, w$R_2 = 0.1142$ and the Flack parameter = −0.004(14). Crystallographic data of **1** have been deposited in the Cambridge Crystallographic Data Center (deposition number CCDC 1416589†).

Eutypellazine E (**5**) was obtained colorless crystal from MeOH using the vapor diffusion method. The orthorhombic crystal (0.30 × 0.25 × 0.05) was measured on Bruker D8 Advance single crystal X-ray diffractometer with Cu-Kα radiation at 99.9 K. Crystal data of **5**: empirical formula $C_{20.21}H_{22.84}N_2O_{5.40}S_2$, $M = 444.37$; space group $P2_12_12_1$, unit cell dimensions $a = 14.08776(18)$ Å, $b = 15.8916(19)$ Å, $c = 27.9520(4)$ Å, $\alpha = \beta = \gamma = 90.00°$, $V = 6257.82(14)$ Å, $Z = 12$, $D_{calcd} = 1.1415$ mg m^{-3}, $\mu = 2.639$ mm^{-1}, $F(000) = 2800$; a total of 42 403 reflections were collected in the range of $6.40° < 2\theta < 142.14°$, of which 11 963 independent reflections [$R_{(int)} = 0.0396$ (inf-0.9 Å)] were used for the analysis. The structure was solved by the direct methods with the SHELXL-97 program and refined using full-matrix least-squares difference Fourier techniques. The final R indexes [all data] gave $R_1 = 0.0463$, w$R_2 = 0.1175$ and the Flack parameter = 0.015(12). Crystallographic data of **5** have been deposited in the Cambridge Crystallographic Data Center (deposition number CCDC 1416590†).

Upon crystallization from MeOH–H_2O (100 : 1) using the vapor diffusion method, colorless crystals were obtained for eutypellazine F (**6**). The orthorhombic crystal (0.40 × 0.35 × 0.25) was measured on Bruker D8 Advance single crystal X-ray diffractometer with Cu-Kα radiation at 101.8 K. Crystal data of **6**: empirical formula $C_{19}H_{24}N_2O_7S_2$, $M = 456.52$; space group $P2_12_12_1$, unit cell dimensions $a = 9.5541(9)$ Å, $b = 13.1555(17)$ Å, $c = 15.7112(6)$ Å, $\alpha = \beta = \gamma = 90.00°$, $V = 1974.7(3)$ Å, $Z = 4$, $D_{calcd} = 1.536$ mg m^{-3}, $\mu = 2.864$ mm^{-1}, $F(000) = 960$; a total of 6784 reflections were collected in the range of $8.76° < 2\theta < 141.64°$, of which 3711 independent reflections [$R_{(int)} = 0.0199$ (inf-0.9 Å)] were used for the analysis. The structure was solved by the direct methods with the SHELXL-97 program and refined using full-matrix least-squares difference Fourier techniques. The final R indexes [all data] gave $R_1 = 0.0300$, w$R_2 = 0.0772$ and the Flack parameter = 0.007(13). Crystallographic data of **6** have been deposited in the Cambridge Crystallographic Data Center (deposition number CCDC 1416591†).

Eutypellazine G (**7**) was obtained colorless crystal from MeOH–H_2O (50 : 1) using the vapor diffusion method. The monoclinic crystal (0.15 × 0.15 × 0.10) was measured on Bruker D8 Advance single crystal X-ray diffractometer with Cu-Kα radiation at 103.3 K. Crystal data of **7**: empirical formula $C_{20}H_{30}N_2O_8S_2$, $M = 490.58$; space group $P2_12_12_1$, unit cell dimensions $a = 9.16165(19)$ Å, $b = 9.5804(2)$ Å, $c = 25.5833(6)$ Å, $\alpha = \beta = \gamma = 90.00°$, $V = 2245.52(9)$ Å, $Z = 4$, $D_{calcd} = 1.451$ mg m^{-3}, $\mu = 2.589$ mm^{-1}, $F(000) = 1040$; a total of 7719 reflections were collected in the range of $6.92° < 2\theta < 142.36°$, of which 4256 independent reflections [$R_{(int)} = 0.0280$ (inf-0.9 Å)] were used for the analysis. The structure was solved by the direct methods with the SHELXL-97 program and refined using full-matrix least-squares difference Fourier techniques. The final R indexes [all data] gave $R_1 = 0.0414$, w$R_2 = 0.1015$ and the Flack parameter = −0.003(18). Crystallographic data of **7** have been deposited in the Cambridge Crystallographic Data Center (deposition number CCDC 1416592†).

Eutypellazine H (**8**) was obtained colorless crystal from MeOH using the vapor diffusion method. The orthorhombic crystal (0.60 × 0.25 × 0.25) was measured on Bruker D8 Advance single crystal X-ray diffractometer with Cu-Kα radiation at 102.4 K. Crystal data of **8**: empirical formula $C_{19}H_{22}N_2O_6S_2$, $M = 438.51$; space group $P2_12_12_1$, unit cell dimensions $a = 8.27744(17)$ Å, $b = 10.60684(20)$ Å, $c = 21.3739(4)$ Å, $\alpha = \beta = \gamma = 90.00°$, $V = 1876.57(6)$ Å, $Z = 4$, $D_{calcd} = 1.552$ mg m^{-3}, $\mu = 2.948$ mm^{-1}, $F(000) = 920$; a total of 7441 reflections were collected in the range of $8.28° < 2\theta < 142.24°$, of which 3517 independent reflections [$R_{(int)} = 0.0238$ (inf-0.9 Å)] were used for the analysis. The structure was solved by the direct methods with the SHELXL-97 program and refined using full-matrix least-squares difference Fourier techniques. The final R indexes [all data] gave $R_1 = 0.0330$, w$R_2 = 0.0827$ and the Flack parameter = −0.008(13). Crystallographic data of **8** have been deposited in the Cambridge Crystallographic Data Center (deposition number CCDC 1416593†).

2.6. Anti-HIV bioassay

293T cells were cultured at 37 °C in a 5% CO_2 humidified atmosphere and split twice a week. The vector pNL4.3-Luc was generated by cloning the luciferase gene (Thermo Fisher

Scientific) in the HIV-1 proviral clone pNL4.3. Plasmid pNL4.3-Ren was generated by cloning the renilla gene (Promega) in the Luc site of pNL4.3-Luc (NIH AIDS Reagent Program). Infectious supernatants were obtained from $Ca_3(PO4)_2$ transfection on 293T cells of plasmid pNL4.3-Ren. These supernatants were used to infect cells in the presence or absence of the compounds to be evaluated. Anti-HIV activity quantification was performed 48 h postinfection. Briefly, cells were lysed with 100 μL of buffer. Relative luminescence units (RLUs) were obtained in a luminometer (Berthold Detection Systems) after the addition of substrate to cell extracts. Viability was performed in parallel treated cells with the same concentrations of compound. After 48 h, cell viability was evaluated with the CellTiter Glo (Promega) assay system following the manufacturer's specifications. Inhibitory concentrations 50% (IC_{50}) and cytotoxic concentrations 50% (CC_{50}) were calculated using GraphPad Prism software.

2.7. *In vitro* latent HIV reactivating assay

For flow cytometry-bases screening, the J-Lat A2 cell line containing an integrated HIV-1 long terminal repeat (LTR) luciferase reporter construct but expressing no Tat was used. The J-Lat A2 cells were grown in Dulbecco's modification of eagle's medium (DMEM) (Thermo Fisher Scientific) supplemented with 10% fetal bovine serum (Aleken Biologicals), 2 mM L-glutamine (Invitrogen), 4500 mg mL^{-1} glucose, and antibiotic solution (0.2% kanamycin, 0.2% streptomycin, and 0.12% penicillin) (Sigma Aldrich) at 37 °C under 5% CO_2 atmosphere. The DMEM replaced every date until cells grew to 90% confluency from explants and then using Tyrisin (Invitrogen) to dissociate them. These cultures of J-Lat A2 cells were then dispensed into 24-well plates at 1×10^5 cells per mL per well 24 h prior to the test compounds treatment and incubated at 37 °C under 5% CO_2 condition. The test compounds (100 μM for each), two positive controls prostratin (5 μM), and SAHA (2.5 μM), and negative control DMSO (10 μL) were added to per well. After 48 h incubation, cells were rinsed and resuspended by phosphate-buffered saline (PBS) (Thermo Fisher Scientific) and then the flow cytometry was used to detect EGFP-positive cells. Cytotoxicities of all compounds were measured by the Promega CellTiter kit (CellTiter-Glo® Reagent) following the manufacturer's instructions in 96-well plates incubated with test compounds at 37 °C for 48 h.

3. Results and discussion

3.1. Structure elucidation of new compounds

The EtOAc extract of the fermentation broth of *Eutypella* sp. MCCC 3A00281 was examined by the HPLC-ESIMS, which featured an array of TDKP-based derivatives. Detailed chromatographic separation including semipreparative HPLC purification resulted in the isolation of 15 TDKP analogues including 13 new compounds (Fig. 1).

Eutypellazine A (**1**) was isolated as white monoclinic crystals. Its molecular formula was established as $C_{19}H_{20}N_2O_5S_2$ by the HRESIMS (*m*/*z* 421.0887 $[M + H]^+$) and NMR data. The IR absorptions at 3370, 1713 and 1648 cm^{-1} suggested the presence of hydroxy and carbonyl functionalities. The ^1H and ^{13}C NMR data (Tables 1 and 2) were characteristic of a diketopiperazine-based derivative, while analyses of ^1H–^1H COSY, HSQC and HSBC data revealed the presence of a 6/5/6/5/6-membered pentacyclic diketopiperazine skeleton, structurally related to the coexisted epicoccin I.[15] The spin system coupled the protons from the olefinic proton H-5 (δ_H 5.98) to H-9 (δ_H 4.78), while the HMBC correlations from H-9 to C-2 (δ_C 74.7), C-3 (δ_C 38.3), C-4 (δ_C 134.1), and C-5 (δ_C 119.6) and from H-5 to C-3 and C-9 (δ_C 69.3) assigned a dihydroindoline for rings A–B, in which a hydroxy substitution at C-8 (δ_C 73.9) was deduced by the COSY relationship between H-8 (δ_H 4.66) and a D_2O exchangeable proton OH-8 (δ_H 5.43). Extensive analyses of the 2D NMR data uncovered rings D–E to be a perhydroindole, in which the location of a ketone group at C-5′ (δ_C 207.9) and a hydroxy group at C-8′ (δ_C 66.1) was evident from the HMBC correlations from C-5′ to H_2-3′, H-4′, and H_2-6′ and the COSY relationship between H-8′ (δ_H 4.03) and OH-8′ (δ_H 6.21). In addition, the chemical shifts of a methyl group at δ_H 2.24 (3H, s)/δ_C 14.5 were characteristic of a thiomethyl group, which was located at C-2 on the basis of the HMBC correlation between the methyl protons and C-2. The second sulfur element was bonded across C-2′ (δ_C 70.1) and C-7′ (δ_C 41.8) to form a thioether bridge on the basis of the HMBC correlation between H-7′ (δ_H 3.74) and C-2′.

The relative configurations of **1** were established by the coupling constants and the NOE data. The $J_{H\text{-}8/H\text{-}9}$ value (13.8 Hz) in association with the NOE interaction between OH-8 and H-9 was indicative of *trans* orientation of H-8 toward H-9. The observation of the NOE correlations from CH_3S (δ_H 2.24) to H-8 and H-8′, and from H-9′ to OH-8′ and H-4′ assigned the same face of thiomethyl group as H-8 and H-8′, while the *cis* fusion of rings D and E was deduced by the NOE interactions from H-4′ and H-9′ to OH-8′. The thioether orientation in opposite face to H-9′ was due to the NOE interaction between OH-8′ and H-7′ (Fig. 2). The absolute configurations of the stereogenic centers were determined by the X-ray diffraction experiment, while the Flack parameter (−0.004(14)) using Cu-Kα reflection measurement unambiguously determined 2*R*, 8*S*, 9*S*, 2′*R*, 4′*R*, 7′*R*, 8′*R*, and 9′*S* configurations, respectively (Fig. 3).

Analyses of the 2D NMR data revealed the structure of eutypellazine B (**2**) closely related to **1**. The distinction was observed in ring E, where a ketone at C-5′ of **1** to be replaced by a hydroxy group, as recognized by the COSY relationship between the D_2O exchangeable proton at δ_H 4.85 (OH) and H-5′ (δ_H 4.31), in addition to the HMBC correlations from the OH proton to C-4′, C-5′ (δ_C 61.5), and C-6′. Comparison of the NOE data and coupling constants indicated that both **2** and **1** share the same relative configurations in rings A–C, whereas the NOE interaction between H-5′/H-9′ and OH-5′/H-8′ (Fig. 2) assigned the opposite face of OH-5′ and OH-8′. Considering the absolute configuration established for **1** by X-ray data, the similar ECD data such as the positive Cotton effects at 230 and 270 nm which reflected the orientation of the thiomethyl group and thioether assumed both **2** and **1** sharing the same absolute configurations. Thus, the stereogenic center C-5′ in **2** was suggested to have the *S* configuration.

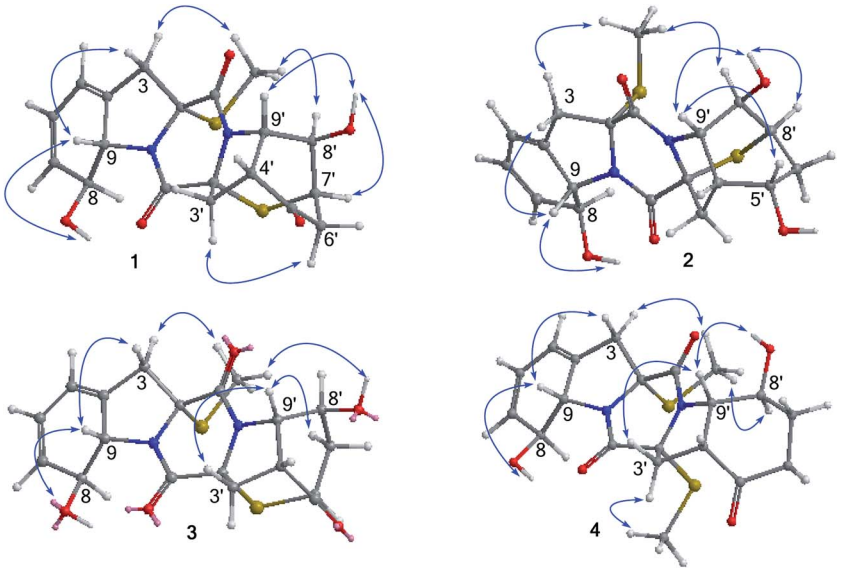

Fig. 2 Key NOE correlations of **1**–**4**.

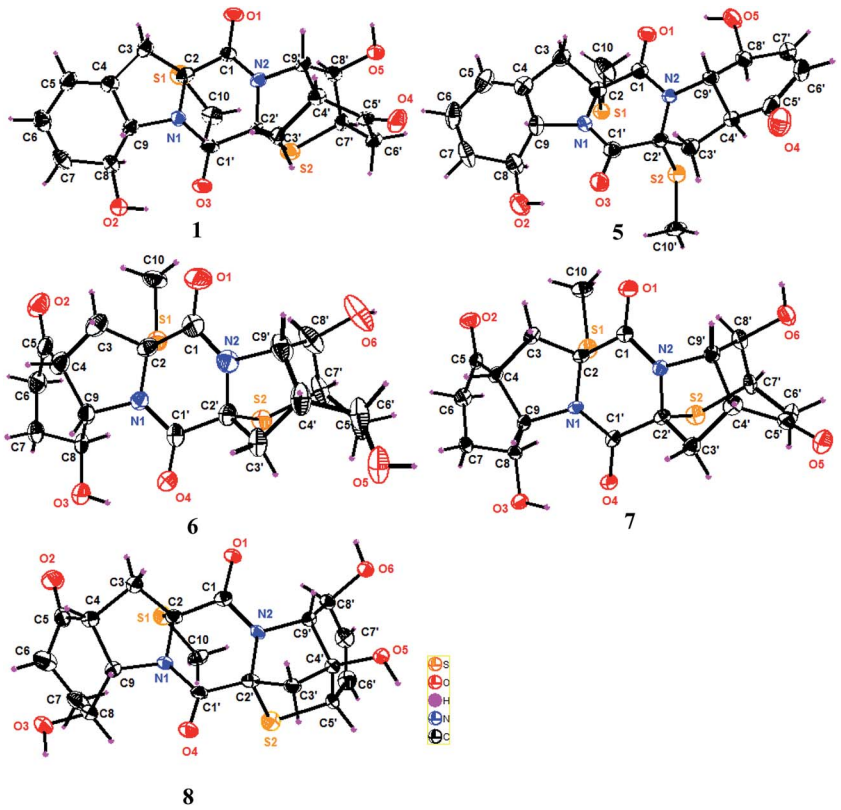

Fig. 3 ORTEP plots of the X-ray crystal structures of **1** and **5**–**8**.

Eutypellazine C (**3**) has the same molecular formula as that of **1**, as determined by the HRESIMS and NMR data. The 2D NMR data indicated that the partial structure of **3** regarding rings A–C was identical to that of **1**, while rings D and E presented as a perhydroindoline unit related to that of **1**. The COSY and HMQC data conducted H-6′ (δ_H 3.64) to be a methine proton instead of H-7′ ring E of **1**. This assignment was evident from the COSY relationship from H_2-7′ (δ_H 2.53, 2.69) to H-6′ and H-8′ (δ_H 4.50). The HMBC correlation between H-6′ and C-2′ confirmed the connection of a thioether bond across C-2′ and C-6′. The closely similar NOE data (Fig. 2) and coupling constants allowed the assignment of the relative configurations of **3** to be

the same as those of **1**. The positive Cotton effects at 220 and 307 nm and the negative Cotton effect at 255 nm were attributed to 2*R* configuration, whereas the positive Cotton effect at 270 nm was induced by the $\pi \rightarrow \pi^*$ transition of conjugated hexadiene.[17] Thus, the remaining stereogenic centers of **3** were assigned as 2*R*, 8*S*, 9*S*, 2′*R*, 4′*R*, 6′*S*, 8′*S*, and 9′*S*, respectively.

The molecular formula of eutypellazine D (**4**) was established as $C_{20}H_{24}N_2O_5S_2$ by the HRESIMS (*m*/*z* 437.1201 $[M + H]^+$) and NMR data. Comparison of the NMR (Tables 2 and 4) and ESIMS data indicated that the structure of **4** closely related to *ent*-epicoccin G.[15] The distinction was attributed to ring A, where the 2D NMR data assigned a 8-hydroxycyclohexadiene with the same moiety as that of **1**. Based on the modified Mosher's method,[18] compound **4** was esterified by the (*R*)- and (*S*)-MPA to form MPA esters **4a** and **4b**. Calculation of the chemical shift values ($\Delta\delta^{RS} = \delta_R - \delta_S$) resulted in a *S* configuration for C-8 and C-8′ (Fig. 4). In combination with the NOE interactions (Fig. 2), the absolute configurations of the remaining chiral centers were determined. These assignments were also supported by the negative Cotton effect at 262 nm, which was in agreement with 2*R*/2′*R* configurations for TDKPs bearing two *S*-methyl groups.[17]

Analyses of the 2D NMR data revealed that eutypellazine E (**5**) was a 6′,7′-dehydrogenated analogue of **4**. This assignment was evident from the similar NMR data of both **4** and **5**, with the exception of the presence of two olefinic protons at δ_H 6.06 (H-6′) and δ_H 6.91 (H-7′) in addition to the HMBC correlations from H-6′ and H-7′ to C-5′ and C-8′. The NOE relationships revealed the same relative configuration in rings A–C of both **4** and **5**. However, the NOE interactions between H-9′/OH-8′ and H-4′/H-8, in association with $J_{H\text{-}4'/H\text{-}9'}$ value (13.3 Hz) conducted a *trans* fusion of rings D and E. This assignment was further supported by the X-ray single crystal diffraction data using Flack parameter (0.015(12)) (Fig. 3), which deduced the absolute configurations to be 2*R*, 8*S*, 9*S*, 2′*R*, 4′*S*, 8′*S*, and 9′*S*, respectively.

Eutypellazine F (**6**) has a molecular formula of $C_{19}H_{22}N_2O_6S_2$ as determined by the HRESIMS and NMR data. Comparison of the NMR data in association with the 2D NMR data resulted in the partial structure regarding rings C–E to be the same as that of **1**. The distinction was recognized in ring A, where the location of a ketone group at C-5 was based on the COSY relationships of the spin system from H_2-3 to H-9, and the HMBC correlations from C-5 to H_2-3, H-4, H_2-6, H_2-7, and H-9. The relative configurations of **6** were determined by the NOE relationships, while the absolute configurations were determined by the single crystal X-ray diffraction data using the Flack parameter (0.007(13)) as obtained by Cu-Kα diffraction to assign 2*R*, 4*R*, 8*S*, 9*S*, 2′*R*, 4′*R*, 7′*R*, 8′*R*, and 9′*S*, respectively (Fig. 3).

Comparison of the NMR data (Tables 3 and 4) indicated that the partial structure of rings A–C in eutypellazine G (**7**) is the same as that of **6**, while the second partial structure in rings C-E of **7** was identical to that of **2**. The absolute configurations of **7** were unequivocally assigned as 2*R*, 4*R*, 8*S*, 9*S*, 2′*R*, 4′*R*, 5′*S*, 7′*R*, 8′*R*, and 9′*S*, respectively, on the basis of the Flack parameter −0.003(18), which was obtained by the X-ray Cu-Kα crystallographic experiment.

The 2D NMR data assigned eutypellazine H (**8**) to be a thiodiketopiperazine with the partial structure of rings A–C being the same as that of **7**, whereas the structure of rings C-E agreed with that of epicoccin I.[15] The absolute configurations **8** were determined by the single crystal X-ray crystallographic data with the Flack parameter −0.008(13), as obtained by the X-ray Cu-Kα experiment, indicating 2*R*, 4*R*, 8*S*, 9*S*, 2′*R*, 4′*S*, 5′*S*, 8′*S*, and 9′*R*, respectively.

The molecular formula of eutypellazine I (**9**) was established as $C_{19}H_{18}N_2O_3S$ on the basis of the HRESIMS (*m*/*z* 355.1120, $[M + H]^+$) and NMR data. The ^1H and ^{13}C NMR data (Tables 3 and 4) of **9** were closely related to those of coexisted emethacin A,[19] whereas the aromatic ring A presented a phenolic proton and an ABCD spin system instead of the mono-substituted aromatic ring of the known counterpart. The aromatic spin system among H-5 (δ_H 7.12, d, $J = 7.3$ Hz), H-6 (δ_H 6.70, t, $J = 7.3$ Hz), H-7 (δ_H 7.04, t, $J = 7.5$ Hz), and H-8 (δ_H 6.80, d, $J = 8.0$ Hz), in association with the HMBC correlations from H_2-3 to C-9 (δ_C 156.0), clarified **9** to be a 9-hydroxyemethacin A. This assignment was supported by the negative sign and the similar value of the specific rotation of both **9** and emethacin A.

Analyses of the NMR and HRESIMS data conducted eutypellazine J (**10**) to be a 9-hydroxyemethacin B, while the distinction was attributed to the aromatic ring A where an ABCD spin system among H-5 (δ_H 6.30), H-6 (δ_H 6.25), H-7 (δ_H 6.89), and H-8 (δ_H 6.67) and the HMBC correlations from H_2-3 (δ_H 3.01, 3.09) to C-4 (δ_C 122.3), C-5 (δ_C 130.0), and C-9 (δ_C 155.6) were observed in the ^1H–^1H COSY and HMBC spectra. The similar magnitude and the same sign of the specific rotation of **10** ($[\alpha]_D^{25}$ −128, MeOH) and emethacin B ($[\alpha]_D^{25}$ −168, $CHCl_3$)[19] assumed **10** possessing 2*R*/2′*R* configurations.

Comparison of the NMR data (Tables 3 and 4) indicated the structure of eutypellazine K (**11**) to be closely related to emethacin B. The distinction was found by the absence of a thiomethyl group and the deshielded C-2′ (δ_C 81.9) in the NMR spectra of **11**. In addition, a D_2O exchangeable proton (δ_H 6.60, s) showed the HMBC correlations with C-1′ (δ_C 167.5), C-2′, and C-3′ (δ_C 44.8), confirming C-2′ of **11** to be substituted by a hydroxy group to replace a thiomethyl group of emethacin B. The NOE interaction between CH_3S and OH-2′ assigned the spatial approximation of both functional groups. In addition, the negative specific rotation of **11** ($[\alpha]_D^{25}$ −165, MeOH) which was contributed by the chiral centers at C-2 and C-2′ and was comparable to that of **10**, suggested 2*R*/2′*R* configurations.

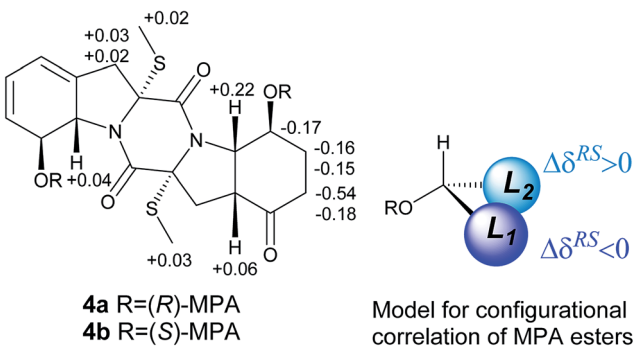

Fig. 4 $\Delta\delta^{RS}$ ($\delta_R - \delta_S$) values of the MPA esters of **4** in $CDCl_3$.

Eutypellazine L (**12**) was determined to have a planer structure to be the same as that of **11**, based on the 2D NMR and HRESIMS data. The distinction was observed by the deshielded C-2′ (δ_C 82.7) and the lower magnitude of the specific rotation ($[\alpha]_D^{25}$ −80) in comparison with those of **11**. Since the hydroxylated and methoxylated diatretol with 2*S* and 2′*S* configurations exhibited positive specific rotation ($[\alpha]_D^{25}$ +42, MeOH),[20] the lowering value of the specific rotation of **11** was derived by the 2′*S* contribution.

Eutypellazine M (**13**) has a molecular formula of $C_{19}H_{20}N_2O_4$ as provided by the HRESIMS (*m*/*z* 339.1342 $[M - H]^-$) and NMR data. Analyses of the NMR data revealed that **13** structurally related to **11** with the exception of the substitution at C-2, in which a methoxy group (δ_H 2.06/δ_C 49.1) instead of a thiomethyl group was recognized to position at C-2. This assignment was supported by the HMBC correlation between the methoxy protons and C-2 (δ_C 87.4). The remarkable shielded protons of MeO (δ_H 2.06) was due to the location of the MeO group under the shielded zone of the nucleus, while the NOE interaction between MeO and OH-2′ (δ_H 5.85) clarified the same orientation of both MeO and OH-2′. Thus, the negative specific rotation of **13** ($[\alpha]_D^{25}$ −72) was in agreement with 2*R* configuration.

The known compounds were determined as epicoccin I[15] and epicoccin A,[6] on the basis of comparison their spectra data with those reported in the literatures.

3.2. Anti-HIV assay

The isolated compounds were tested for their inhibitory effects against human immunodeficiency virus type 1 (HIV-1) replication. Anti-HIV screening was performed by the pNL4.3.Env-.Luc co-transfected 293T cells. Before bioassay, all compounds were tested for their cytotoxicity toward 293T cells, while the tested compounds showed low cytotoxicity with CC_{50} > 100 μM. Compounds in a single dose of 20 μM showing more than 50% of HIV-1 inhibition were subjected to IC_{50} measurement. As shown in Table 5, most of the tested compounds exerted inhibitory effects, while compound **5** showed the most inhibitory effect. A preliminary structure–activity relationship study revealed that the analogues with thiomethyl group at C-2/C-2′ (**4** and **5**) showed more active than those with sulfide bridge (**1–3**, **6–8**) in the pentacyclic thiodiketopiperazines. Comparison of the inhibitory effect between **4** and **5** revealed a double bond at C-6′/C-7′ in **5** enhancing the activity. In regard to compounds **9–13**, the analogues with thiomethyl group at C-2/C-2′ (**10**) showed more effect than those with hydroxyl substitution (**11–12**), whereas the analogue with methoxy/hydroxyl substitution at C-2/C-2′ dramatically reduced the activity.

In addition, compound **10** and epicoccin A showed the reactivation on latent HIV-1 transcription with dose-dependent manner, whereas the remaining compounds exerted inactive in a dose of 100 μM. As shown in Fig. 5, compound **10** and epicoccin A showed the reactivation activities at 80 μM, which were comparable to the positive controls prostratin (5 μM) and SAHA (2.5 μM). Latent HIV reservoirs are the primary hurdle to eradicate human immunodeficiency virus by the highly active antiretroviral therapy (HAART), because the residual provirus harbored in cellular reservoirs quickly rebound when treatment is interrupted.[21,22] One promising strategy to expunge HIV-1 infection is to reactive latent viral reservoirs in combination with HAART.[23,24] Thus, finding new latency reactivating agents with noncytotoxic, clinically effective treatment of HIV infections is urgently needed.

Table 5 Evaluation of anti-HIV activity of selected compounds[a]

Compounds	IC_{50} + SD (μM)	CC (μM)
1	14.8 + 1.2	>100
2	11.5 + 0.8	>100
3	10.7 + 1.3	>100
4	8.7 + 0.5	>100
5	3.2 + 0.4	>100
6	16.6 + 0.5	>100
7	18.2 + 1.3	>100
8	13.3 + 0.6	>100
9	6.7 + 2.1	>100
10	4.9 + 1.1	>100
11	5.8 + 0.7	>100
12	5.9 + 0.9	>100
13	>20	>100
EFV	0.1	>100

[a] IC_{50} (inhibitory concentration 50%) and CC_{50} (cytotoxic concentration 50%).

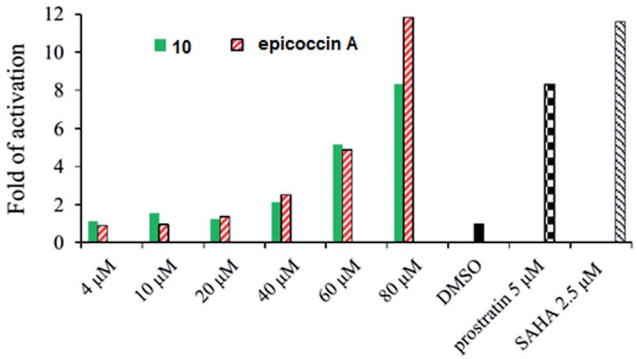

Fig. 5 Reactivating effects of **10** and epicoccin A on latent HIV-1 expression in J-Lat A2 cell. Positive control: prostratin and SAHA; negative control: DMSO. The compounds were detected by flow cytometry for the EGFP-positive cells. The activity detected in cells treated with DMSO was set to 1 and the values shown in figure were mean from two independent experiments.

4. Conclusion

Previous investigation of *Eutypella* fungi inhabited in terrestrial and marine habitats have uncovered diverse terpenoids[25–28] and cytosporin-related compounds.[29,30] This is the first report of thiodiketopiperazine-type alkaloids to be derived from *Eutypella* sp., suggesting the presence of diverse biogenetic synthetic pathways in a fungal strain and the distinct synthetic pathway to be activated from a fungal strain inhabited in different location. In addition, the present work not only enriched the numbers of new analogues in thiodiketopiperazine family, also

extended the pharmaceutical usage of thiodiketopiperazines to anti-HIV activities. The potent anti-HIV effects of the new compounds suggested that they may serve as new scaffolds for structural modification to be developed as a group of new anti-HIV candidates. The reactivation on latent HIV-1 expression induced by **10** and epicoccin A suggested that both compounds may be applied as new latency reactivating agents, which are rarely found from natural products.

Acknowledgements

This work was supported by the grants of National High Technology and Science 973 program (2015CB755906), and NSFC (81630089, 41376127).

References

1 R. W. Timothy and M. W. Robert, *Nat. Prod. Rep.*, 2014, **31**, 1376–1404.
2 G. C. Horace, H. Karst, H. L. Robert and H. A. Byron, *Agric. Biol. Chem.*, 1991, **55**, 2037–2042.
3 Y. Zhang, S. Liu, Y. Che and X. Liu, *J. Nat. Prod.*, 2007, **70**, 1522–1525.
4 H. Guo, B. Sun, H. Gao, X. Chen, S. Liu, X. Yao, X. Liu and Y. Che, *J. Nat. Prod.*, 2009, **72**, 2115–2119.
5 L. Meng, X. Li, C. Lv, C. Huang and B. Wang, *J. Nat. Prod.*, 2014, **77**, 1921–1927.
6 Y. Sun, K. Takada, Y. Takemoto, M. Yoshida, Y. Nogi, S. Okada and S. Matsunaga, *J. Nat. Prod.*, 2012, **75**, 111–114.
7 C. Guo, H. Yeh, Y. Chiang, J. F. Sanchez, S. Chang, K. S. Bruno and C. C. C. Wang, *J. Am. Chem. Soc.*, 2013, **135**, 7205–7213.
8 H. S. Daniel, H. Andreas, H. Thorsten, A. B. Axel and H. Christian, *J. Am. Chem. Soc.*, 2014, **136**, 11674–11679.
9 R. Tan, P. R. Jensen, P. G. Williams and W. Fenical, *J. Nat. Prod.*, 2004, **67**, 1374–1382.
10 F. Kong, Y. Wang, P. Liu, T. Dong and W. Zhu, *J. Nat. Prod.*, 2014, **77**, 132–137.
11 C. Takahashi, Y. Takai, Y. Kimura, A. Numata, N. Shigematsu and H. Tanaka, *Phytochemistry*, 1995, **38**, 155–158.
12 L. H. Meng, P. Zhang, X. M. Li and B. G. Wang, *Mar. Drugs*, 2015, **13**, 276–287.
13 M. Saka, S. Palasarn, P. Rachtawee, S. Vimuttipong and P. Kongsaeree, *Org. Lett.*, 2005, **7**, 2257–2260.
14 H. J. Lee, J. H. Lee, B. Y. Hwang, H. S. Kim and J. J. Lee, *Arch. Pharmacal Res.*, 2001, **25**, 397–401.
15 J. Wang, G. Ding, L. Fang, J. Dai, S. Yu, Y. Wang, X. Chen, S. Ma, J. Qu, S. Xu and D. Du, *J. Nat. Prod.*, 2010, **73**, 1240–1249.
16 J. Wang, W. He, X. Qin, X. Wei, X. Tian, L. Liao, S. Liao, B. Yang, Z. Tu, B. Chen, F. Wang, X. Zhou and Y. Liu, *RSC Adv.*, 2015, **5**, 68736–68742.
17 J. Wang, N. Jiang, J. Ma, S. Yu, R. Tan, J. Dai, Y. Si, G. Ding, S. Ma, J. Qu, L. Fang and D. Du, *Tetrahedron*, 2013, **69**, 1195–1201.
18 F. Freire, F. Calderon, J. M. Seco, A. Fernandez-Mayoralas, E. Quinoa and R. Riguera, *J. Org. Chem.*, 2007, **72**, 2297–2301.
19 N. Kawahara, K. Nozawa, S. Nakajima, M. Yamazaki and K. Kawai, *Heterocycles*, 1989, **29**, 397–402.
20 A. Alberto, C. Silvia, N. Gianluca, V. M. Stefano and V. P. Orso, *Liebigs Ann.*, 1996, 1875–1877.
21 B. León, G. Navarro, B. J. Dickey, G. Stepan, A. Tsai, G. S. Jones, M. E. Morales, T. Barnes, S. Ahmadyar, M. Tsiang, R. Geleziunas, T. Cihlar, N. Pagratis, Y. Tian, H. Yu and R. G. Linington, *Org. Lett.*, 2015, **17**, 262–265.
22 A. Jordan, D. Bisgrove and E. Verdin, *EMBO J.*, 2003, **22**, 1868–1877.
23 E. J. Mejia, S. T. Loveridge, G. Stepan, A. Tsai, G. S. Jones, T. Barnes, K. N. White, M. Drašković, K. Tenney, M. Tsiang, R. Geleziunas, T. Cihlar, N. Pagratis, Y. Tian, H. Yu and P. Crews, *J. Nat. Prod.*, 2014, **77**, 618–624.
24 Z. Li, J. Guo, Y. Wu and Q. Zhou, *Nucleic Acids Res.*, 2013, **41**, 277–287.
25 W. Pongcharoen, V. Rukachaisirikul, S. Phongpaichit, N. Rungjindamai and J. Sakayaroj, *J. Nat. Prod.*, 2006, **69**, 856–858.
26 L. Sun, D. Li, M. Tao, Y. Chen, F. Dan and W. Zhang, *Mar. Drugs*, 2012, **10**, 539–550.
27 M. Isaka, S. Palasarn, W. Prathumpai and P. Laksanacharoen, *Chem. Pharm. Bull.*, 2011, **59**, 1157–1159.
28 X. Lu, J. Liu, X. Liu, Y. Gao, J. Zhang, B. Jiao and H. Zheng, *J. Antibiot.*, 2014, **67**, 171–174.
29 M. Isaka, S. Palasarn, S. Lapanun, R. Chanthaket, N. Boonyuen and S. Lumyong, *J. Nat. Prod.*, 2009, **72**, 1720–1722.
30 M. L. Ciavatta, M. P. Lopez-Gresa, M. Gavagnin, R. Nicoletti, E. Manzo, E. Mollo, Y. Guo and G. Cimino, *Tetrahedron*, 2008, **64**, 5365–5369.

